On the approximation of transport properties in structured materials using momentum-transfer theory

On the approximation of transport properties in structured materials using momentum-transfer theory

G J Boyle[1,3]**, R D White**[1]**, R E Robson**[1]**, S Dujko**[2]
and Z Lj Petrović[2]

[1] ARC Centre for Antimatter-Matter Studies, School of Engineering and
Physical Sciences, James Cook University, Townsville 4810, Australia
[2] Institute of Physics, University of Belgrade, Pregrevica 118, 11080 Belgrade,
Serbia
E-mail: gregory.boyle@jcu.edu.au

Abstract. In this paper, we present a fluid model for electrons and positrons in structured and soft-condensed matter utilizing dilute gas phase cross-sections together with a structure factor for the medium. Generalizations of the Wannier energy and Einstein (Nernst–Townsend) relations to account for coherent scattering effects present in soft-condensed matter are presented along with new expressions directly relating transport properties in the dilute gas and the structured matter phases. The theory is applied to electrons in a benchmark Percus–Yevick model and positrons in liquid argon, and the accuracy is tested against a multi-term solution of Boltzmann's equation (White and Robson 2011 *Phys. Rev.* E **84** 031125).

[3] Author to whom any correspondence should be addressed.

Contents

1. Introduction

For many technological applications and basic areas of research in physics and chemistry, an understanding of charged particle transport in soft-condensed matter and structured mediums, such as liquids and dense gases, is required. Examples include the development of new and better insulators and semi-conductors in the microprocessor industry [2, 3], improvements to positron-based imaging techniques in medicine [4], radiation damage modelling [5, 6] and liquid particle detection chambers [7]. The drive towards improved modelling of these systems and devices has spurred renewed interest in understanding the fundamental physical processes involved, including accurate knowledge and implementation of charged particle cross-sections, material structure and transport theories.

The modelling of charged particle behaviour in condensed systems is more complicated than the equivalent gas phase situation, since a full statistical elucidation in which both kinetic and configurational processes contribute to the total energy is required, unlike the gas or solid state where one of the processes dominates [8]. The approach to incorporating this inherent structure in the framework of modern kinetic theory was proposed by Cohen and Lekner [9], using structure functions introduced by Hove [10] that contain all the necessary information about the excitations in the single-scatterer approximation. The status of the field was detailed in a recent review by Sakai [8]. Even more recently, White *et al* [1, 11] have formulated a new modification to the Boltzmann equation describing electron and positron transport in structured and soft-condensed matter. They solved the new kinetic equation using a multi-term solution technique that overcomes some of the limitations associated with previous solution techniques [8, 9]. The new kinetic equation represents the fundamental equation from which macroscopic transport properties of interest can be determined from microscopic information such as collision cross-sections and structure factors [9, 10].

The integro-differential nature of the kinetic equation renders finding a general solution for the velocity (phase-space) distribution function a computationally expensive task. In this paper, we set aside the task of finding the phase-space distribution function, and focus on the kinetic theory at a semi-quantitative level by considering a fluid approach. Here, fluid equations are generated by taking low-order moments of the kinetic equation, which essentially represent continuity, momentum and energy balance equations [12–15]. Whereas it is difficult to gain physical insight directly from the full Boltzmann equation, the moment approach allows one to obtain analytic relations between measurable quantities and hence a direct physical

understanding of the relationships between these properties. This procedure has a long history in the kinetic theory of gases [16, 17]. While there are many and varied techniques to close the set of moment equations and approximate the moments of the collision integral (see [11, 18] for discussions), we believe that momentum-transfer theory (MTT) (see the textbook discussion [19]) represents the most transparent and internally consistent method. It is exact in the benchmark case of point-charged induced dipole interactions, and the prescriptions for improved accuracy are clear [13, 20]. While the primary aim of MTT initially was to furnish relationships between measurable quantities (e.g. the Wannier energy relations, generalized Einstein (Nernst–Townsend) relations (GER), etc), more recently it has been demonstrated to provide transport properties in good qualitative and semi-quantitative agreement with more rigorous treatments, such as Boltzmann equation solutions and Monte Carlo simulations [11, 15, 18, 20–26].

While there exists a large body of literature dedicated to the measurement and calculation of scattering cross-sections and transport properties for the dilute gas phase, the same cannot be said for the structured and soft-condensed phases. One aim of our work is to capitalize on this body of literature in the gas phase by adapting and applying it where possible. Our previous work focused on the implementation of gas phase cross-sections to consider such systems [1, 11], and here we extend our aim to consider the calculation of transport properties in structured and soft-condensed materials from transport properties measured or calculated in the dilute gas phase limit.

We begin this paper with a review of the kinetic theory in section 2.1, which adapts a knowledge of gas phase scattering cross-sections to consider charged particle transport in soft-condensed matter. Based on this theory, a hierarchy of moment equations is then developed in section 2.2. Well-known relationships in dilute gaseous systems, such as Wannier's energy relation, GER and effective field concepts, are generalized to structured systems where coherent scattering effects are operative in section 2.3, and numerical results are presented for electrons and positrons in model and real systems. Finally, in an effort to improve our fluid equation results and capitalize on the existing gas phase literature, the relationships between transport properties in dilute gas phase systems and those in soft-condensed phases are outlined in section 2.4, and numerical results are compared to those derived previously.

2. Theory

2.1. Kinetic theory

The fundamental equation describing a swarm of light, charged particles moving through a gaseous or soft-condensed matter medium subject to an electric field, $\mathbf{E}$, is the Boltzmann kinetic equation for the phase-space distribution function $f \equiv f(\mathbf{r}, \mathbf{v}, t)$ [8]:

$$\left(\frac{\partial}{\partial t} + \mathbf{v} \cdot \nabla + \frac{q\mathbf{E}}{m} \cdot \frac{\partial}{\partial \mathbf{v}} \right) f = -J(f), \tag{1}$$

where $\mathbf{r}$, $\mathbf{v}$, q and m are the position, velocity, charge and mass of the swarm particle, respectively. The right-hand side describes the effect of collisions on the distribution function f at a fixed position and velocity. Essentially, the Boltzmann equation is an equation of continuity in phase space. The collision integral can be separated as

$$J(f) = J_{\text{elas}}(f) + J_{\text{inel}}(f) + J_{\text{Ps}}(f) + \cdots, \tag{2}$$

which then accounts for all possible scattering processes, such as elastic collisions, inelastic collisions, positronium formation, etc, through appropriate cross-sections. An important distinction between coherent and incoherent scattering processes needs to be made for the consideration of charged particle transport in structured media.

The most general view of charged particle interactions with a medium is that of a wave representing the charged particle being scattered by the medium as a whole. A first approximation to the scattering is the 'single-scatterer approximation' [10] in which the scattered wave is the coherent sum of the contributions of many scattering centres in the molecule, which interfere to effectively produce a diffraction pattern of the medium [1]. The interference effects arising from coherent scattering processes can significantly affect the charged particle transport within the media. When the de Broglie wavelength of the charged particle is small compared to the medium's inter-particle spacing, the charged particle wave is essentially only sampling a single medium particle during a collision, and structure effects are suppressed. The problem then reduces to the dilute gas phase limit, for which our model for transport is well understood. The effects of coherent scattering manifest themselves in the J_{elas} term of (2).

From the definition of the double differential cross-section, $d^2\sigma/(d\mathbf{k}\, d\omega)$, the rate of change of a property Ψ due to collisions can be found [1]:

$$\left(\frac{\partial \Psi}{\partial t}\right)_{coll} = n_0 \int d\mathbf{v}\, v f(\mathbf{v}) \int d\omega' \int d\Omega_{\mathbf{k}'} \left[\Psi(\mathbf{v}) - \Psi'(\mathbf{v}')\right] \frac{d^2\sigma}{d\mathbf{k}'\, d\omega'}, \tag{3}$$

where ω and $\mathbf{k}$ denote the charged particle angular frequency and wave number, respectively, and $d\Omega_{\mathbf{k}'}$ is the solid angle centred on the scattered wave. n_0 is the neutral number density. Undashed and dashed quantities refer to properties before and after interaction, respectively. The double differential cross-section can be expressed in terms of the single-particle differential cross-section, $\left(\frac{d\sigma}{d\omega'}\right)^{(lab)}$, which depends purely on the properties of the interaction, and the dynamic structure factor, $S(\Delta\mathbf{k}, \Delta\omega)$ [10], which encompasses properties of the medium only, i.e.

$$\frac{d^2\sigma}{d\mathbf{k}'\, d\omega'} = \left(\frac{d\sigma}{d\omega'}\right)^{(lab)} S(\Delta\mathbf{k}, \Delta\omega), \tag{4}$$

where $\Delta\mathbf{k} \equiv \mathbf{k} - \mathbf{k}'$ is the change in the wave vector, and $\Delta\omega \equiv \omega - \omega'$ is the change in energy due to interaction with the medium. The dynamic structure factor is the space and time Fourier transform of the Van Hove time-dependent, generalized, pair-distribution function and contains all the necessary information about the excitations of the system in the single-scatterer approximation.

A more directly useful property that can be derived from the dynamic structure factor is the 'static structure factor', $S(\mathbf{K})$:

$$S(\mathbf{K}) \equiv \int_{-\infty}^{\infty} d\Omega\, S(\mathbf{K}, \Omega). \tag{5}$$

Equation (5) is only valid if $\mathbf{K}$ and Ω are independent. To enforce this, along with other sum rules, terms are expanded about $K = 2k\sin(\chi/2) = (2mv/\hbar)\sin(\chi/2)$, i.e. the momentum transfer in an elastic collision in which the particle is scattered through an angle χ [1, 10]. The differential cross-section, Σ, modified to account for coherent scattering is then found to be [27]

$$\Sigma(v, \chi) = \sigma(v, \chi) S\left(\frac{2mv}{\hbar}\sin\left(\frac{\chi}{2}\right)\right). \tag{6}$$

For dilute gases, $S(\Delta\mathbf{k}) \to 1$, and it follows that $\Sigma(v, \chi) \to \sigma(v, \chi)$ and the expressions reduce to their dilute gaseous form, as required.

2.2. Fluid equations and momentum-transfer theory (MTT)

A full and general solution to (1) can be achieved only numerically [1, 11]. A fluid equation treatment can yield approximate quantitative results and, importantly, can furnish analytic relationships between physically measurable properties. The problem of solving the Boltzmann equation for f in phase space is replaced by a low-order set of approximate (velocity) moment equations of f [12, 13, 15, 28–30]. The set of moment equations is found by multiplying the modified Boltzmann equation (1) by an arbitrary property of swarm particle velocity, $\Phi(\mathbf{v})$, and integrating over all velocities:

$$\frac{\partial}{\partial t}\left[n\langle\Phi(\mathbf{v})\rangle\right] + \nabla \cdot \left[n\langle\mathbf{v}\Phi(\mathbf{v})\rangle\right] - n\frac{q}{m}\left\langle\mathbf{E}\cdot\frac{\partial}{\partial\mathbf{v}}\Phi(\mathbf{v})\right\rangle = -\int\Phi(\mathbf{v})J(f)\mathrm{d}\mathbf{v}, \tag{7}$$

$$= C_\Phi, \tag{8}$$

where $\langle\rangle$ represents the average over swarm particle velocity, and the negative on the right-hand side of (7) indicates the rate of loss of that quantity due to collisions with the medium. If one assumes that $\Phi(\mathbf{v})$ equals 1, $m\mathbf{v}$, $\frac{1}{2}mv^2$, etc in succession, the above generates an infinite chain, a full solution of which would be equivalent to knowing f. In practice, one must truncate the chain, and generally for light particles only the first three moment equations are required. Setting $\Phi(\mathbf{v})$ to be equal to 1, $m\mathbf{v}$ and $\frac{1}{2}mv^2$ yields the continuity, momentum and energy balance equations, respectively:

$$\frac{\partial n}{\partial t} + \nabla \cdot n\mathbf{v} = C_1, \tag{9}$$

$$\frac{\partial}{\partial t}[nm\langle\mathbf{v}\rangle] + \nabla \cdot [nm\langle\mathbf{v}\mathbf{v}\rangle] - nm\mathbf{a} = C_{m\mathbf{v}}, \tag{10}$$

$$\frac{\partial}{\partial t}\left[n\left\langle\frac{1}{2}mv^2\right\rangle\right] + \nabla \cdot \left[n\left\langle\frac{1}{2}mv^2\mathbf{v}\right\rangle\right] - nm\mathbf{a}\cdot\langle\mathbf{v}\rangle = C_{\frac{1}{2}mv^2}. \tag{11}$$

MTT provides a way of evaluating the collision terms [19], and the exact form will be detailed below. For now, it suffices to say that the collision frequencies are assumed to be slow-varying functions of energy. The Taylor series representation,

$$\nu(\epsilon) = \nu(\bar{\epsilon}) + (\epsilon - \bar{\epsilon})\nu'(\bar{\epsilon}) + \cdots, \tag{12}$$

about some reference energy, $\bar{\epsilon}$, at which the dominant contribution to the average occurs, can then be assumed to converge rapidly. It is assumed that the appropriate reference energy is average energy $\langle\epsilon\rangle$. For conservative collisional processes, such as elastic and inelastic scattering, only the first term of the expansion (12) is generally considered. However, when energy-dependent non-conservative processes, such as positronium formation, positron annihilation and electron-induced ionization, are required in the description, the derivative term in (12) becomes the leading term and must be kept.

The connection between experiment and theory is generally given by the continuity equation,

$$\frac{\partial n(\mathbf{r}, t)}{\partial t} + \nabla \cdot \Gamma(\mathbf{r}, t) = S(\mathbf{r}, t), \tag{13}$$

where $\Gamma = n \langle \mathbf{v} \rangle$ is the swarm particle flux, n is the charged particle density and S represents a source or sink term arising from the presence of non-conservative collisional processes. If the gradient of the swarm number density is also assumed to be small, and we are far from boundaries, sources or sinks, the 'hydrodynamic regime' applies, and one can apply the density gradient expansion of the phase-space distribution function [29]. The space–time dependence of all properties is then effectively projected onto functionals of the number density. Projecting out the space and time dependence of the average energy, $\epsilon(\mathbf{r}, t)$, and flux, $\Gamma(\mathbf{r}, t)$, in the same manner, we have, respectively,

$$\epsilon(\mathbf{r}, t) = \left\langle \frac{1}{2} m v^2 \right\rangle = \epsilon + \gamma \cdot \frac{\nabla n}{n} + \cdots, \tag{14}$$

$$\Gamma(\mathbf{r}, t) = n \langle \mathbf{v} \rangle = n\mathbf{W} - \mathbf{D} \cdot \nabla n + \cdots, \tag{15}$$

where ϵ is the mean energy of the swarm and γ is the gradient energy parameter [31]. It should be noted that in the case of positron transport the skewing of the swarm profile may become extreme and terms beyond the second order one in the expansion may be required in equation (14) [21]. Fick's law (15) defines the 'flux drift velocity' $\mathbf{W}$ and 'flux diffusion tensor' $\mathbf{D}$. These are distinct from the 'bulk' transport coefficients [18, 32, 33], which are not considered here. If the hydrodynamic regime has not been reached, then the space–time dependence of the distribution function cannot be projected onto the number density, and transport coefficients are not meaningful quantities. A complete, non-hydrodynamic solution is then required.

Using the explicit form of the collision operators used in [1, 27] and applying the relevant approximations from MTT, the set of moment equations (9)–(11) in the hydrodynamic regime yield for a steady-state swarm of light particles, $m \ll m_0$, the following hierarchy of coupled equations:

$$\mathbf{W} = \frac{q\mathbf{E}}{m \left(\tilde{\nu}_m + \frac{2}{3} \epsilon \nu'_A \right)}, \tag{16}$$

$$\epsilon = \frac{3}{2} k T_0 + \frac{1}{2} m_0 \mathbf{W}^2 \frac{\tilde{\nu}_m}{\nu_m} - \frac{\Omega}{\nu_e} - \frac{2}{3} \epsilon^2 \frac{\nu'_A}{\nu_e}, \tag{17}$$

$$\left(\tilde{\nu}_m + \frac{2}{3} \epsilon \nu'_A \right) \mathbf{D} = \frac{\mathrm{d}}{\mathrm{d}\epsilon} \left(\tilde{\nu}_m + \frac{2}{3} \epsilon \nu'_A \right) \mathbf{W} \gamma + \frac{2}{3} \frac{\epsilon}{m} \mathbf{I}, \tag{18}$$

$$\left[1 + \frac{\nu'_m}{\nu_m} \left(\epsilon - \frac{3}{2} k T_0 - \frac{1}{2} m_0 \mathbf{W}^2 \frac{\tilde{\nu}'_m}{\nu'_m} \right) + \frac{\Omega'}{\nu_e} + \frac{1}{\nu_e} \frac{\mathrm{d}}{\mathrm{d}\epsilon} \left(\frac{2}{3} \epsilon^2 \nu'_A \right) \right] \gamma$$

$$= -m_0 \frac{\tilde{\nu}_m}{\nu_m} \mathbf{W} \cdot \mathbf{D} - \mathbf{Q}. \tag{19}$$

The effect of attachment enters the balance equations through the derivative, ν'_A. It has also been assumed that, for light particles, random motion dominates directed motion, i.e. $\langle v^2 \rangle \geqslant \langle \mathbf{v} \rangle^2$. The

IOP Institute of Physics Φ DEUTSCHE PHYSIKALISCHE GESELLSCHAFT

average momentum and transfer collision frequencies

$$\nu_m(\epsilon) = \nu_m^{\text{elas}}(\epsilon) + \nu_m^{\text{inel}}(\epsilon) \tag{20a}$$

$$= \sum_j n_{0j}\sqrt{\frac{2\epsilon}{m}}\sigma_m(j,j;\epsilon) + \sum_{\substack{j,j'\\j\neq j'}} n_{0j}\sqrt{\frac{2\epsilon}{m}}\sigma_m(j,j';\epsilon) \tag{20b}$$

$$= \sum_{j,j'} n_{0j}\sqrt{\frac{2\epsilon}{m}}\sigma_m(j,j';\epsilon), \tag{20c}$$

$$\nu_e(\epsilon) = \frac{2m}{m_0}\nu_m(\epsilon), \tag{20d}$$

$$\tilde{\nu}_m(\epsilon) = \tilde{\nu}_m^{\text{elas}}(\epsilon) + \nu_m^{\text{inel}}(\epsilon) \tag{20e}$$

$$= \sum_j n_{0j}\sqrt{\frac{2\epsilon}{m}}\tilde{\sigma}_m(j,j;\epsilon) + \sum_{\substack{j,j'\\j\neq j'}} n_{0j}\sqrt{\frac{2\epsilon}{m}}\sigma_m(j,j';\epsilon), \tag{20f}$$

$$\nu_A(\epsilon) = \sum_{j,j'} n_{0j}\sqrt{\frac{2\epsilon}{m}}\sigma_A(j,j';\epsilon) \tag{20g}$$

represent the dilute gas phase momentum and energy transfers, soft-condensed momentum transfer and attachment collision frequencies, respectively, and are all prescribed functions of the mean energy defined in the centre of mass frame. The terms σ_m, $\tilde{\sigma}_m$ and σ_A represent the momentum-transfer cross-sections for dilute gaseous and soft-condensed mediums and the attachment cross-section, respectively. Ω represents the energy lost in inelastic collisions in one elastic energy transfer collisional time, ν_e^{-1}, and is given by

$$\Omega(\epsilon) = \sum_I \Delta\epsilon_I \left(\langle \overrightarrow{\nu_I}(\epsilon) \rangle + \langle \overleftarrow{\nu_I}(\epsilon) \rangle \right). \tag{21}$$

The inelastic channels I are governed by threshold energies ϵ_I, and collision frequencies for inelastic and superelastic processes, $\overrightarrow{\nu_I}(\epsilon)$ and $\overleftarrow{\nu_I}(\epsilon)$, respectively.

Equations (16) and (17) represent coupled nonlinear differential equations for the drift velocity $\mathbf{W}$ and mean energy ϵ, which serve as inputs into the linear coupled differential equations (18) and (19) for the diffusion coefficients and gradient energy parameters. The heat flux, $\mathbf{Q}$, is found from higher-order moments, and so an assumption needs to be made to achieve closure. In this work we neglect $\mathbf{Q}$, which is generally a safe assumption under hydrodynamic conditions, but not always [34]. For a further discussion on the heat flux, see [18].

From this system of equations, structure-modified generalizations of well-known dilute gas phase results, such as Wannier's energy relation [17], GER [20] and others, can be made, as detailed below.

2.3. Standard MTT

In the preceding section, the system of equations (16)–(19) were derived for homogeneous and first-order inhomogeneous transport coefficients valid in soft-condensed matter. The aim

of this section is to develop semi-analytic relationships between dilute gas phase microscopic information, such as cross-sections and the medium structure factor, and soft-condensed phase macroscopic transport coefficients. To illustrate the technique, we limit ourselves to the simple case of a steady, spatially uniform swarm subject to an electric field, undergoing elastic and particle-loss processes only with a background medium. In this case, $\nu_m = \nu_m^{elas}$, $\tilde{\nu}_m = \tilde{\nu}_m^{elas}$ and $\Omega = 0$.

2.3.1. Drift velocity and mean energy.   If 'effective collision frequencies' are defined by

$$\tilde{\nu}_{eff} = \tilde{\nu}_m + \tfrac{2}{3}\epsilon \nu'_A, \tag{22}$$

$$\nu_{eff} = \nu_m + \tfrac{2}{3}\epsilon \nu'_A, \tag{23}$$

then equations (16) and (17) simplify to

$$W = \frac{qE}{m\tilde{\nu}_{eff}} \tag{24}$$

and

$$\epsilon = \frac{3}{2}kT_0 + \frac{1}{2}m_0 W^2 \frac{\tilde{\nu}_m}{\nu_m} - \frac{2}{3}\epsilon^2 \frac{\nu'_A}{\nu_e}, \tag{25}$$

which can be combined as

$$\epsilon = \frac{3}{2}kT_0 + \frac{1}{2}m_0 \left(\frac{qE}{m}\right)^2 \frac{\tilde{\nu}_m}{\tilde{\nu}_{eff}^2 \nu_m} - \frac{2}{3}\epsilon^2 \frac{\nu'_A}{\nu_e}. \tag{26}$$

Equation (25) is a generalization of the well-known Wannier energy relation [17] in dilute gas transport theory, which is frequently used empirically to produce the approximate mean energy from measured drift velocities [19]. From (26), it is clear that, given the knowledge of the dilute gas phase cross-sections for the necessary processes and the structure factor of the medium, the above nonlinear expressions can be solved for the soft-condensed phase mean energy and drift velocity numerically [35, 36].

It is well known in gas transport theory that, for some energy profiles, the inclusion of inelastic or non-conservative scattering cross-sections can cause regions in which the flux drift velocity decreases despite an increase in the applied electric field [19]. The conditions for the occurrence of this phenomena, known as 'negative differential conductivity' (NDC), have been investigated previously [15, 21, 34, 37, 38]. For a structured medium there is a new type of NDC [27] that does not require inelastic collisions or non-conservative processes, i.e. purely a consequence of the medium structure. NDC is characterized by a decrease in the drift velocity W despite an increase in the magnitude of applied electric field E, i.e.

$$\frac{dW}{dE} < 0. \tag{27}$$

For simplicity, we assume elastic collisions only and take the cold gas approximation, $T = 0\,K$, such that the drift and mean energy equations (24) and (25), respectively, become

$$W = \frac{qE}{m\tilde{\nu}_m} \tag{28}$$

and

$$\epsilon = \frac{1}{2}m_0 W^2 \frac{\tilde{\nu}_m}{\nu_m}. \tag{29}$$

From these relations it can be shown that

$$\frac{d\epsilon}{d \ln E} \left[1 - \frac{d \ln \left(\frac{\tilde{\nu}_m}{\nu_m} \right)}{d \ln \epsilon} \right] = m_0 W \frac{\tilde{\nu}_m}{\nu_m} \frac{dW}{d \ln E}. \tag{30}$$

Considering the signs of the left-hand side and right-hand side constituents of (30) and noting that $\frac{d\epsilon}{d \ln E} > 0$ when only electric fields are present, it is evident that for structure-induced NDC to occur, the following condition must be met:

$$\frac{d \ln \left(\frac{\tilde{\nu}_m}{\nu_m} \right)}{d \ln \epsilon} > 1. \tag{31}$$

In section 2.3.4, this condition is further explored through numerical investigations.

2.3.2. Diffusion coefficients. The homogeneous transport coefficients found in section 2.3.1 can be used to find first-order inhomogeneous transport coefficients. For the electric field only case considered here, there are two non-zero components of the diffusion tensor: those parallel to the electric field, $D_\parallel$, and those perpendicular, $D_\perp$, given by

$$D_\perp = \frac{2}{3} \frac{\epsilon}{m \tilde{\nu}_{\text{eff}}} \tag{32}$$

and

$$D_\parallel = \frac{2}{3} \frac{\epsilon}{m \tilde{\nu}_{\text{eff}}} + \frac{\tilde{\nu}'_{\text{eff}}}{\tilde{\nu}_{\text{eff}}} W \gamma, \tag{33}$$

where the dash represents an energy derivative. Substituting the parallel component of expression (19) (neglecting the heat flux) into (33) and re-arranging gives

$$D_\parallel = \frac{2}{3} \frac{\epsilon}{m \tilde{\nu}_{\text{eff}}} \left[1 + \frac{m_0 W^2 \frac{\tilde{\nu}'_{\text{eff}}}{\nu_{\text{eff}}} \frac{\tilde{\nu}_m}{\nu_m}}{1 - \frac{1}{2} m_0 W^2 \frac{\partial}{\partial \epsilon} \left(\frac{\tilde{\nu}_m}{\nu_m} \right) + \frac{\partial}{\partial \epsilon} \left(\frac{2}{3} \epsilon^2 \frac{\tilde{\nu}_A}{\nu_e} \right)} \right]^{-1}. \tag{34}$$

This result can be expressed in terms of the mobility, K,

$$K = \frac{W}{E} = \frac{q}{m \tilde{\nu}_{\text{eff}}}, \tag{35}$$

which can then be used in combination with (25) to prove the following identity:

$$\frac{\frac{\partial \ln K}{\partial \ln E}}{\left(1 + \frac{\partial \ln K}{\partial \ln E} \right)} = \frac{-m_0 W^2 \frac{\tilde{\nu}'_{\text{eff}}}{\tilde{\nu}_{\text{eff}}} \frac{\tilde{\nu}_m}{\nu_m}}{1 - \frac{1}{2} m_0 W^2 \frac{\partial}{\partial \epsilon} \left(\frac{\tilde{\nu}_m}{\nu_m} \right) + \frac{\partial}{\partial \epsilon} \left(\frac{2}{3} \epsilon^2 \frac{\tilde{\nu}_A}{\nu_e} \right)}. \tag{36}$$

It follows that equation (34) can be written as

$$\frac{D_\parallel}{D_\perp} = 1 + \frac{\partial \ln K}{\partial \ln E}, \tag{37}$$

which is valid in soft-condensed matter and is of the same form as the well-known GER in dilute gas transport theory [17, 34]. The inclusion of a non-zero heat flux, Q, manifests itself as a correction term in (37) [34].
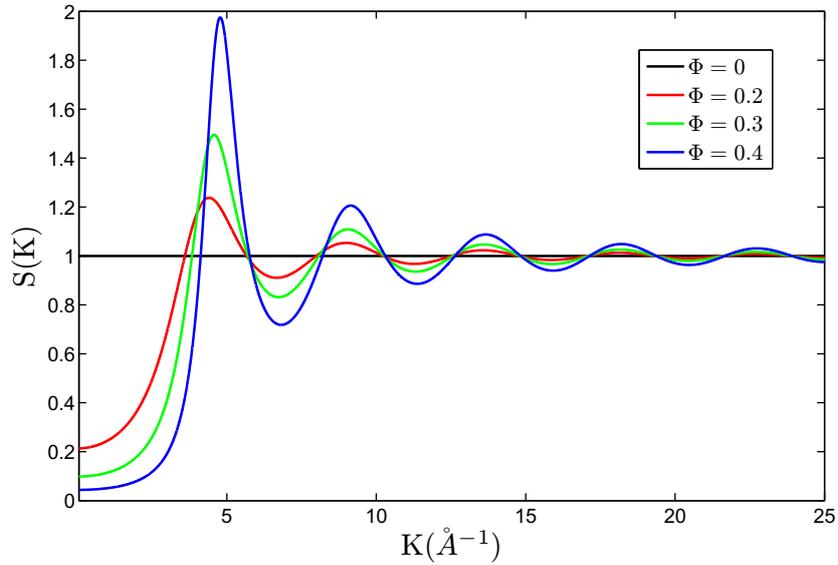
Figure 1. The variation of the static structure factor with momentum exchange K for the Percus–Yevick model (with the Verlet–Weiss correction) for various volume fractions, Φ. ——, $\Phi = 0$; ——, $\Phi = 0.2$; ——, $\Phi = 0.3$; ——, $\Phi = 0.4$.

2.3.3. Benchmark model. In order to investigate the effects of structure on charged particle transport, a model for the structure function is required. For a system of hard-spherical particles, the model of Percus and Yevick (with the Verlet–Weiss correction) [39, 40] provides the appropriate structure behaviour. An important factor is the volume fraction, Φ, which is a measure of how tightly packed the particulates of the media are. Low-volume fractions indicate a larger inter-particle spacing, whereas higher-volume fractions indicate a smaller inter-particle spacing. Figure 1 shows the static structure value, $S(K)$, for different values of Φ. The oscillatory nature exhibited in the structure factor is echoed by the behaviour of the transport coefficients. In the limit $K \to \infty$, $S \to 1$, and the dilute gas case is regained.

In the hard-sphere model, the elastic collision cross-section is constant and isotropic. For isotropic scattering, $\sigma(v, \chi)$ is independent of angle χ and the structure-modified momentum-transfer cross-section, $\tilde{\sigma}_m(v)$, accounting for coherent scattering can be found from

$$\tilde{\sigma}_m(v) = \sigma_m(v) s(v), \tag{38}$$

where $s(v)$ is given by

$$s(v) = \frac{1}{2} \int_{-1}^{1} S\left(\frac{2mv}{\hbar} \sin\left(\frac{\chi}{2}\right)\right) (1 - \cos \chi) \, d(\cos \chi). \tag{39}$$

It should be noted that the assumption of isotropy is for simplicity in illustrating the technique and is by no means a necessity (see [27]). The details of the model implemented, for electrons or positrons, are as follows:

$$\sigma_m = 6 \times 10^{-20} \, \mathrm{m}^2,$$

$$m_0 = 4 \, \mathrm{amu},$$
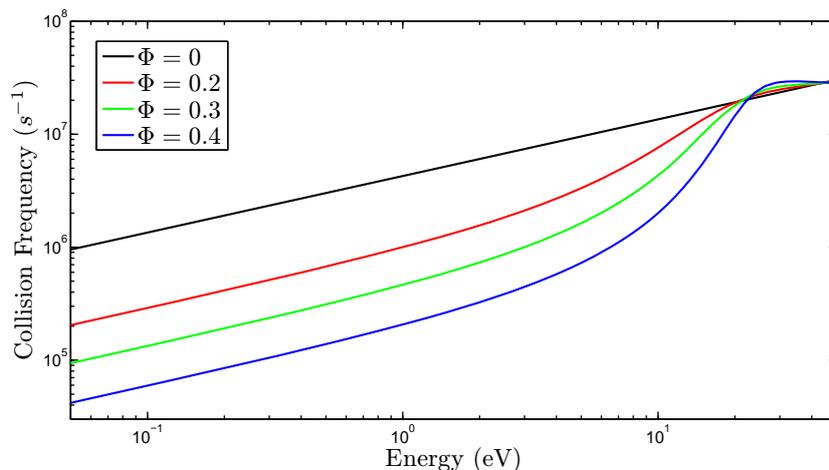
$$T_0 = 0 \, \mathrm{K}.$$

Figure 2. The energy variation of elastic the collision frequency, for various volume fractions Φ, for a dense gas of hard spheres. ——, $\Phi = 0$ ——, $\Phi = 0.2$ ——, $\Phi = 0.3$ —— $\Phi = 0.4$.

The dilute gas and dense gas momentum-transfer collision frequencies for this model as a function of the volume fraction are shown in figure 2. Physically, one expects that as the energy increases, and hence the de Broglie wavelength decreases, the effects of coherent scattering are reduced and the structure-modified profiles converge on the dilute gas phase profile. This is reflected in figure 2.

2.3.4. Mean energy and drift velocity. The spatially homogeneous transport coefficients, i.e. mean energy and drift velocity, were calculated from (16) and (17) for the hard-sphere model. In figures 3 and 4, the variation of swarm mean energy and drift velocity, respectively, with reduced electric field E/n_0 is displayed for the fluid model approach and compared with those of the Boltzmann solution. The fluid model predictions are qualitatively correct and exhibit satisfactory quantitative agreement, generally to within 10–20% of the Boltzmann equation solution results. In regions where the structure-modified momentum-transfer collision frequency varies rapidly with energy, the associated errors are increased. This is consistent with the approximations associated with the low-order truncation of (12) associated with MTT. It is evident that the presence of structure in the medium causes a significant difference between the two sets of coefficients. Coherent scattering effects generally act to reduce the momentum transfer, thus enhancing the field's ability to pump energy and momentum into the system. The enhancements in the mean energy and drift velocity due to enhanced coherent scattering effects then follow. At high fields the profiles converge to the dilute gas phase profile, a reflection of the decrease in the associated de Broglie wavelength and subsequent suppression of coherent scattering effects.

Importantly, in figure 4, the fluid model successfully predicts the phenomenon of structure-induced negative differential conductivity (NDC). While NDC has been demonstrated in the past to be a consequence of inelastic [34] or non-conservative [15] processes, its occurrence here is purely a result of including structure effects. In certain field regions an increase in the field leads to a sharp increase in the momentum-transfer cross-section (a reflection of sharp increases in the structure factor) and hence a decrease in drift velocity (for further details of structure-induced
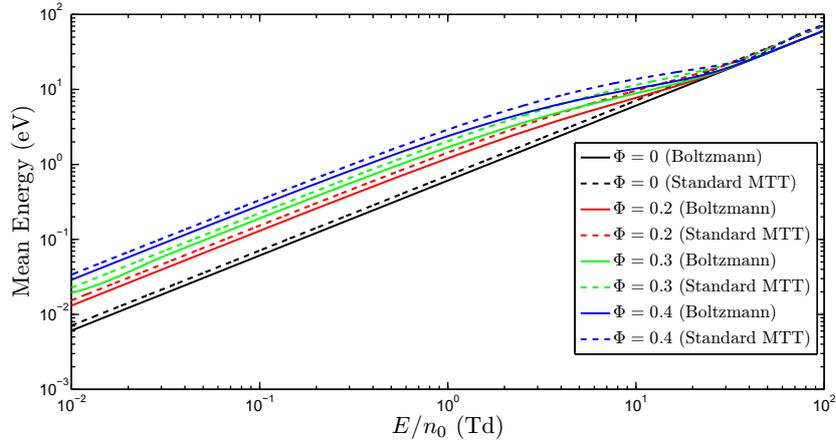
Figure 3. Variation of the swarm mean energy with reduced electric field for various volume fractions Φ for a dense gas of hard spheres. Fluid results are compared with those from a multi-term Boltzmann equation solution [1]. ——, $\Phi = 0$ (Boltzmann); - - - -, $\Phi = 0$ (standard MTT); ——, $\Phi = 0.2$ (Boltzmann); - - - -, $\Phi = 0.2$ (standard MTT); ——, $\Phi = 0.3$ (Boltzmann); - - - -, $\Phi = 0.3$ (standard MTT); ——, $\Phi = 0.4$ (Boltzmann); - - - -, $\Phi = 0.4$ (standard MTT).
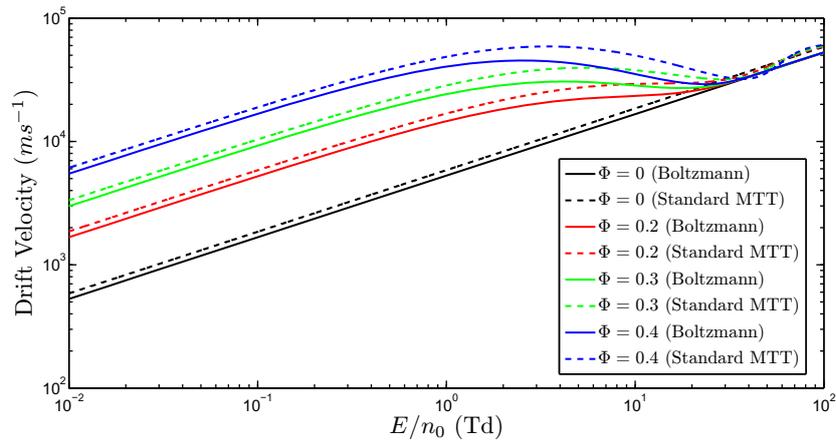

Figure 4. Variation of the swarm flux drift velocity with reduced electric field for various volume fractions Φ for a dense gas of hard spheres. Fluid results are compared with those from a multi-term Boltzmann equation solution [1]. ——, $\Phi = 0$ (Boltzmann); - - - -, $\Phi = 0$ (standard MTT); ——, $\Phi = 0.2$ (Boltzmann); - - - -, $\Phi = 0.2$ (standard MTT); ——, $\Phi = 0.3$ (Boltzmann); - - - -, $\Phi = 0.3$ (standard MTT); ——, $\Phi = 0.4$ (Boltzmann); - - - -, $\Phi = 0.4$ (standard MTT).

NDC, see [1, 27]). A condition for the occurrence of NDC was given in (31), restated differently using (38),

$$\frac{\mathrm{d}\ln s}{\mathrm{d}\ln \epsilon} > 1. \tag{40}$$

Figure 5 shows a log–log plot of energy versus s, as defined in (39), superimposed with straight lines of slope one. It is evident that there are energies for the $\Phi = 0.3$ and $\Phi = 0.4$ profiles for
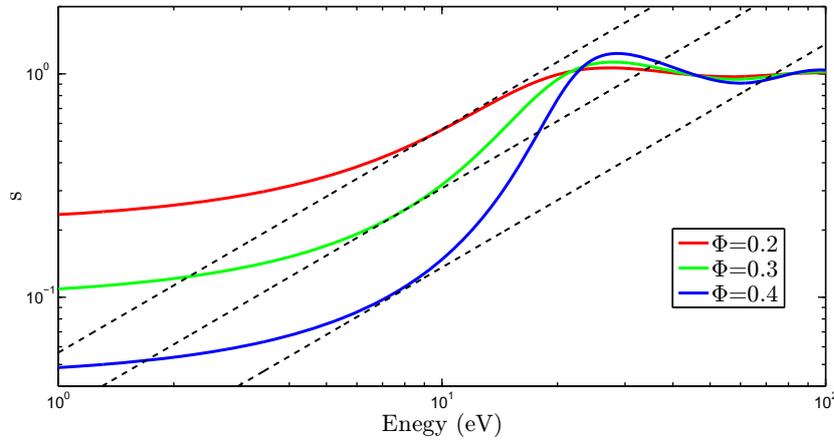
Figure 5. Variation of *s*, as defined in (39), with reduced electric field for various volume fractions Φ for a dense gas of hard spheres. ——, Φ = 0.2; ——, Φ = 0.3; ——, Φ = 0.4.

which the slope of $\log s / \log \epsilon$ exceeds one, but for lower Φ there are none. This coincides with the occurrence of NDC in figure 4 for Φ = 0.3 and Φ = 0.4 and not in the smaller-volume fraction profiles. It can be deduced from (28) that during NDC, a small increase in E is accompanied by a rapid increase in $\tilde{\nu}_m$, resulting in an overall decrease in the drift velocity.

2.3.5. Diffusion coefficients. The phenomenon of anisotropic diffusion is well known for charged particles of all masses in dilute gaseous systems and is now textbook material [19]:

$$\frac{D_\parallel}{D_\perp} = 1 + \frac{\partial \ln K}{\partial \ln E} = \frac{\partial \ln W}{\partial \ln E}. \tag{41}$$

For charged particles interacting with a dilute gas of hard spheres with a constant collision cross-section, $W \sim E^{1/2}$, and hence

$$\frac{D_\parallel}{D_\perp} \simeq 0.5. \tag{42}$$

In figures 6 and 7, we present the variation in the transverse and longitudinal diffusion coefficients, respectively, with reduced electric field as a function of the volume fraction Φ. Figure 6 highlights the effect of coherent scattering on the transverse diffusion coefficient. For low fields, the dense gas diffusion is about two orders of magnitude greater than the dilute gas equivalent, which is successfully predicted by the fluid equations. As the field increases, the fluid approximations depart significantly from the Boltzmann solution, reflecting the regions in the structure factor which vary quickly with energy and violate the assumption made in (12) of a slowly varying collision frequency and subsequent low-order truncation. Extra correction terms may need to be included to account for this. Once the field increases to a point where the collision frequency is less strongly varying with energy, the fluid approximations return to the dense gas phase Boltzmann equation profiles, which converge on the dilute gas profile.

Figure 7 shows the variation of the longitudinal diffusion coefficient with reduced electric field. Comparing with figure 6, the dilute profile for the longitudinal diffusion coefficient is half the value of the transverse diffusion coefficient when considering hard spheres, as predicted by
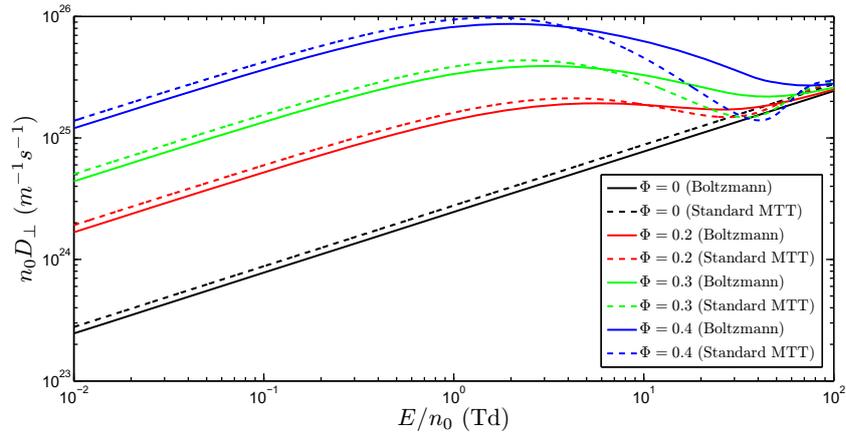
Figure 6. Variation of the transverse diffusion coefficient with reduced electric field for various volume fractions Φ for a dense gas of hard spheres. Fluid results are compared with those from a multi-term Boltzmann equation solution [1]. ——, $\Phi = 0$ (Boltzmann); - - - -, $\Phi = 0$ (standard MTT); ——, $\Phi = 0.2$ (Boltzmann); - - - -, $\Phi = 0.2$ (standard MTT); ——, $\P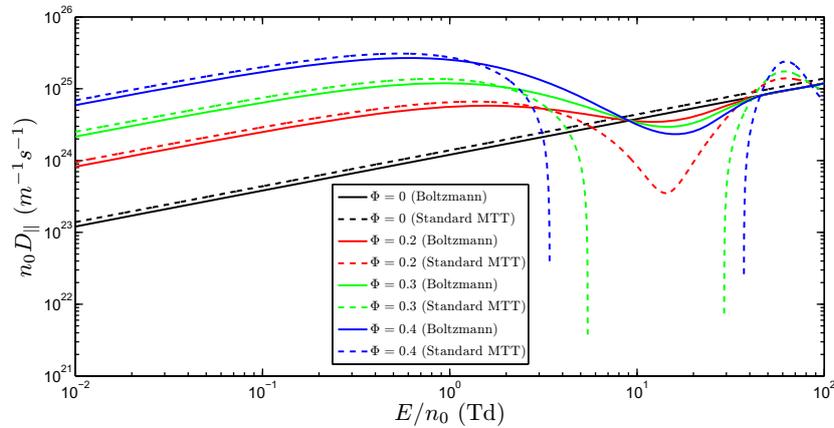hi = 0.3$ (Boltzmann); - - - -, $\Phi = 0.3$ (standard MTT); ——, $\Phi = 0.4$ (Boltzmann); - - - - $\Phi = 0.4$ (standard MTT).

Figure 7. Variation of the longitudinal diffusion coefficient with reduced electric field for various volume fractions Φ for a dense gas of hard spheres. Fluid results are compared with those from a multi-term Boltzmann equation solution [1]. ——, $\Phi = 0$ (Boltzmann); - - - -, $\Phi = 0$ (standard MTT); ——, $\Phi = 0.2$ (Boltzmann); - - - -, $\Phi = 0.2$ (standard MTT); ——, $\Phi = 0.3$ (Boltzmann); - - - -, $\Phi = 0.3$ (standard MTT); ——, $\Phi = 0.4$ (Boltzmann); - - - -, $\Phi = 0.4$ (standard MTT).

the GER (42). When coherent scattering effects are included the ratio of 0.5 is still retained at high and low field strengths. In between the two extremes, the effects of the oscillatory nature of the structure factor on the momentum-transfer collision frequency is exhibited, causing the fluid model to break down entirely for the two largest-volume fractions, $\Phi = 0.3$ and $\Phi = 0.4$,
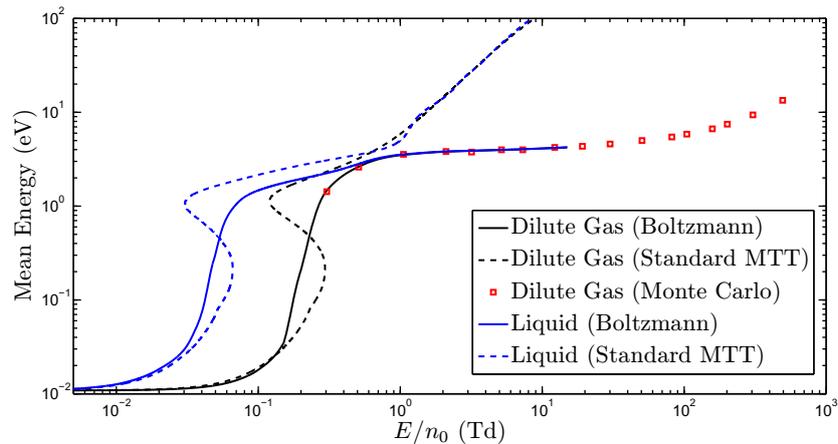
Figure 8. Variation of the swarm mean energy with reduced electric field for dilute gaseous and liquid argon at 84 K. Fluid results are compared with those from a multi-term Boltzmann equation solution [1] and Monte Carlo simulation [21]. ——, Dilute gas (Boltzmann); - - - -, dilute gas (standard MTT); □, dilute gas (Monte Carlo); ——, liquid (Boltzmann); - - - -, liquid (standard MTT).

in the region between about 10 and 20 Td, where the dense gas collision frequency varies sharpest. In this region, we observe that the drift profiles predicted by the fluid approximation in figure 4 exhibit NDC. Consequently, the right-hand side of relation (37) becomes negative and the relation breaks down. Again, extra correction terms in MTT are required to remedy this [34].

2.3.6. Liquid argon. We now apply the theory to the case of positrons in liquid argon at 84 K. This application has been considered previously and data are available for both the dilute gaseous and liquid phases [1, 21, 27]. The semi-analytic expressions (16)–(18) include only elastic and attachment collision effects. As such, it is expected that these will give less accurate results for liquid argon than for the hard-sphere test case, particularly at fields where inelastic effects become significant, but there is a range of fields where these equations are suitable.

Figure 8 details the variation of positron swarm mean energy with the reduced electric field in gaseous and liquid argon. The fluid model gives much less accurate predictions in this scenario as compared to the hard-sphere test model case. The fluid predictions demonstrate peculiar, unphysical behaviour; there are regions in which multiple steady-state mean energies can result from a single reduced electric field strength. Given the occurrence of this behaviour in the dilute gas phase situation as well, it is clearly a consequence of the cross-section behaviour rather than purely a structure effect. Low-order MTT is not sufficient to account for the variation of the collision frequencies. As the field strength increases, the fluid profiles diverge significantly from that of the Boltzmann solution results as neglected inelastic processes become significant.

The same issues are echoed by the drift velocities shown in figure 9; generally bigger errors than the hard-sphere model scenario, peculiar profile behaviour and degeneracy, and large discrepancies when inelastic processes become significant.
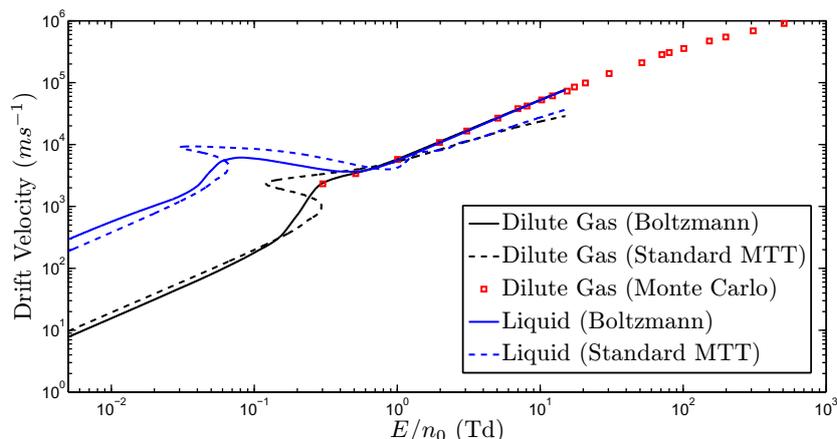
Figure 9. Variation of the swarm flux drift velocity with reduced electric field for dilute gaseous and liquid argon at 84 K. Fluid results are compared with those from a multi-term Boltzmann equation solution [1] and Monte Carlo simulation [21]. —— Dilute gas (Boltzmann); - - - -, dilute gas (standard MTT); □, dilute gas (Monte Carlo); ——, liquid (Boltzmann); - - - -, liquid (standard MTT).

Given the inadequacy of the spatially homogeneous transport property predictions, the higher-order moments, for which these serve as inputs, are not derived. Extra terms in the Taylor series expansion (12) will be required to sufficiently describe positron transport in liquid argon using the standard MTT technique.

In light of the issues experienced using a standard MTT approach, we have developed a modified approach that utilizes the existing dilute gas phase transport coefficient literature to predict transport in the soft-condensed phase and this approach is outlined in the following section.

2.4. Modified MTT

In the preceding section, the relations between dilute gas phase *microscopic* quantities and soft-condensed phase *macroscopic* cross-sections were derived. The aim of this section is to develop semi-analytic relationships between sets of transport coefficients in the dilute gas phase and in the soft-condensed phase, facilitating the prediction of the latter directly from the knowledge of the former and structure information of the medium. Henceforth, tildes will represent transport properties in dense and soft-condensed phases, while those without will represent quantities in the dilute gas phase limit.

The steady-state, spatially homogeneous balance equations, (24) and (25), are restated here for clarity:

$$\tilde{W} = \frac{qE}{m\tilde{\nu}_{\text{eff}}}, \tag{43}$$

$$\tilde{\epsilon} = \frac{3}{2}kT_0 + \frac{1}{2}m_0\tilde{W}^2\frac{\tilde{\nu}_m}{\nu_m} - \frac{2}{3}\tilde{\epsilon}^2\frac{\nu'_A}{\nu_e}. \tag{44}$$

If the inter-particle spacing is large compared to the de Boglie wavelength of the swarm particle, then the static structure factor $S(\Delta \mathbf{k})$ reduces to unity and subsequently $\tilde{\nu}_m \to \nu_m$, regaining the gas phase relations:

$$W = \frac{qE}{m\nu_{\text{eff}}}, \tag{45}$$

$$\epsilon = \frac{3}{2}kT_0 + \frac{1}{2}m_0 W^2 - \frac{2}{3}\epsilon^2 \frac{\nu_{\text{A}}'}{\nu_{\text{e}}}. \tag{46}$$

Comparing (43) and (45),

$$\tilde{W} = W \frac{\nu_{\text{eff}}(\epsilon)}{\tilde{\nu}_{\text{eff}}(\tilde{\epsilon})}, \tag{47}$$

which immediately links the drift velocities and mean energies in the two types of media. Substituting (47) into (44), it follows that

$$\tilde{\epsilon} = \frac{3}{2}kT_0 + \frac{1}{2}m_0 W^2 \left(\frac{\nu_{\text{eff}}(\epsilon)}{\tilde{\nu}_{\text{eff}}(\tilde{\epsilon})}\right)^2 \frac{\tilde{\nu}_m(\epsilon)}{\nu_m(\epsilon)} - \frac{2}{3}\tilde{\epsilon}^2 \frac{\nu_{\text{A}}'(\tilde{\epsilon})}{\nu_{\text{e}}(\tilde{\epsilon})}, \tag{48}$$

which gives the sought expression; a nonlinear relation for the soft-condensed phase mean energy $\tilde{\epsilon}$ purely in terms of the dilute gas phase mean energy ϵ and drift velocity W. In general, this relation must be solved numerically, and results are presented in section 2.4.2. The process for finding soft-condensed phase transport coefficients from dilute gas phase information is then as follows:

(i) Construct ν_m and ν_{A}' by fitting dilute gas phase mean energy and drift velocity according to the functional forms (45) and (46).

(ii) Include coherent scattering effects that, for isotropic scattering, are found simply from $\tilde{\nu}_m = \nu_m s$.

(iii) Solve (48) for soft-condensed phase mean energy, which can then be used to find other condensed-phase transport coefficients.

In the spirit of other popular approaches used in transport physics [16, 23, 41], we seek to represent equation (48) in terms of an 'effective electric field', E_{eff}, i.e. the electric field needed in the dilute gas phase limit to generate the same average energy in the soft-condensed phase:

$$\tilde{\epsilon}(E) = \epsilon(E_{\text{eff}}) \equiv \epsilon. \tag{49}$$

Using (45), equation (46) becomes

$$\epsilon = \frac{3}{2}kT_0 + \frac{1}{2}m_0 \left(\frac{qE_{\text{eff}}}{m\nu_{\text{eff}}}\right)^2 - \frac{2}{3}\epsilon^2 \frac{\nu_{\text{A}}'}{\nu_{\text{e}}}. \tag{50}$$

Combining (50) with (44) yields an expression for the effective electric field strength in terms of the actual applied electric field strength and various collision frequencies evaluated at ϵ:

$$E_{\text{eff}} = E \frac{\nu_{\text{eff}}(\epsilon)}{\tilde{\nu}_{\text{eff}}(\epsilon)} \sqrt{\frac{\tilde{\nu}_m(\epsilon)}{\nu_m(\epsilon)}} \tag{51}$$

$$= E \frac{\nu_{\text{eff}}(\epsilon)}{\tilde{\nu}_{\text{eff}}(\epsilon)} \sqrt{s(\epsilon)}, \tag{52}$$

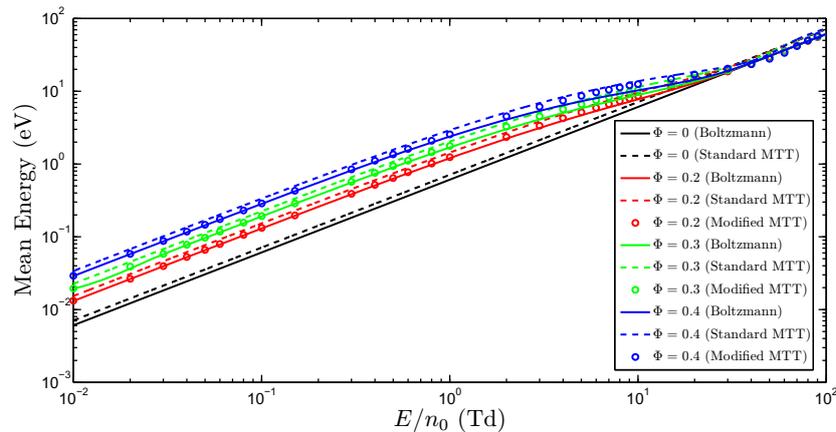**IOP** Institute of Physics **Φ** DEUTSCHE PHYSIKALISCHE GESELLSCHAFT

Figure 10. Variation of the swarm mean energy with reduced electric field for various volume fractions Φ for a dense gas of hard spheres. Fluid results are compared with those from a multi-term Boltzmann equation solution [1]. ——, $\Phi = 0$ (Boltzmann); - - - -, $\Phi = 0$ (standard MTT); ——, $\Phi = 0.2$ (Boltzmann); - - - -, $\Phi = 0.2$ (standard MTT); ○, $\Phi = 0.2$ (modified MTT); ——, $\Phi = 0.3$ (Boltzmann); - - - -, $\Phi = 0.3$ (standard MTT); ○, $\Phi = 0.3$ (modified MTT); ——, $\Phi = 0.4$ (Boltzmann); - - - -, $\Phi = 0.4$ (standard MTT); ○, $\Phi = 0.4$ (modified MTT).

where (52) has been simplified by assuming isotropic scattering. The effective field is nonlinearly dependent on the mean energy, and solving (51) with (50) is mathematically equivalent to solving (48). Effective fields calculated for a simple test model and a more realistic example are presented in section 2.4.2.

Once the mean energy and drift velocity valid in soft-condensed matter have been found, diffusion coefficients can then be derived from the relations given in section 2.3.2. It should be emphasized that the relations for diffusion in the soft-condensed phase require only energy and drift velocity data in the dilute gas phase. This is in the spirit of MTT. However, if one had the dilute gas phase diffusion coefficients one could establish a direct relationship with diffusion coefficients in structured matter.

2.4.1. Benchmark model. The benchmark model of a system of hard spheres described in section 2.3.3 is once again employed.

2.4.2. Mean energy and drift velocity. The spatially homogeneous transport coefficients were calculated from (47) and (48) for the hard-sphere model. Figures 10 and 11 compare the variation of swarm mean energy and drift velocity, respectively, with reduced electric field of the modified MTT approach with those of the standard MTT and Boltzmann solutions. The modified MTT technique generally gives better predictions than the standard MTT. This is a consequence of using 'effective collision frequencies' fitted from the Boltzmann dilute gas phase transport coefficients, which serve to reduce some of the errors involved with MTT. Comments made in section 2.3.3 regarding the qualitative behaviour of the standard MTT mean energy and drift velocity are all still appropriate here.
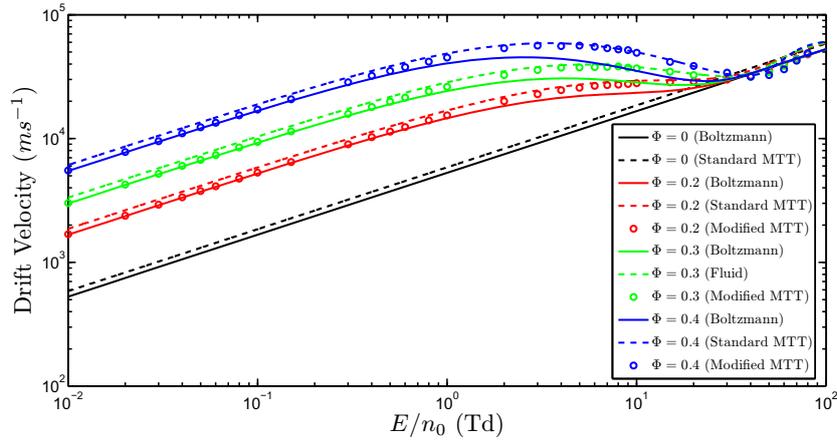
Figure 11. Variation of the swarm flux drift velocity with reduced electric field for various volume fractions Φ for a dense gas of hard spheres. Fluid results are compared with those from a multi-term Boltzmann equation solution [1]. ——, $\Phi = 0$ (Boltzmann); - - - -, $\Phi = 0$ (standard MTT); ——, $\Phi = 0.2$ (Boltzmann); - - - -, $\Phi = 0.2$ (standard MTT); ○, $\Phi = 0.2$ (modified MTT); ——, $\Phi = 0.3$ (Boltzmann); - - - -, $\Phi = 0.3$ (standard MTT); ○, $\Phi = 0.3$ (modified MTT); ——, $\Phi = 0.4$ (Boltzmann); - - - -, $\Phi = 0.4$ (standard MTT); ○, $\Phi = 0.4$ (modified MTT).
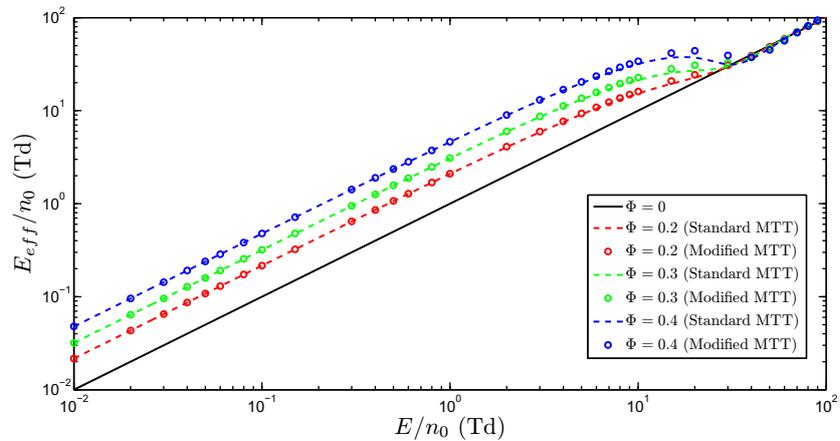

Figure 12. Variation of the reduced effective electric field, E_{eff}, with reduced electric field for various volume fractions Φ for a dense gas of hard spheres. ——, $\Phi = 0$; - - - -, $\Phi = 0.2$ (standard MTT); ○, $\Phi = 0.2$ (modified MTT); - - - -, $\Phi = 0.3$ (standard MTT); ○, $\Phi = 0.3$ (modified MTT); - - - -, $\Phi = 0.4$ (standard MTT); ○, $\Phi = 0.4$ (modified MTT).

In figure 12, the relationship between the actual reduced electric field strength and the effective electric field strength, as described by (51), is shown for the two MTT approaches. Generally, transport in a structured medium requires a lower electric field to generate the same energies and drift velocities as transport in a dilute gas, which is a reflection of the reduction in the momentum transfer due to coherent scattering effects. At high fields, E_{eff} approaches E

IOP Institute of Physics Φ DEUTSCHE PHYSIKALISCHE GESELLSCHAFT
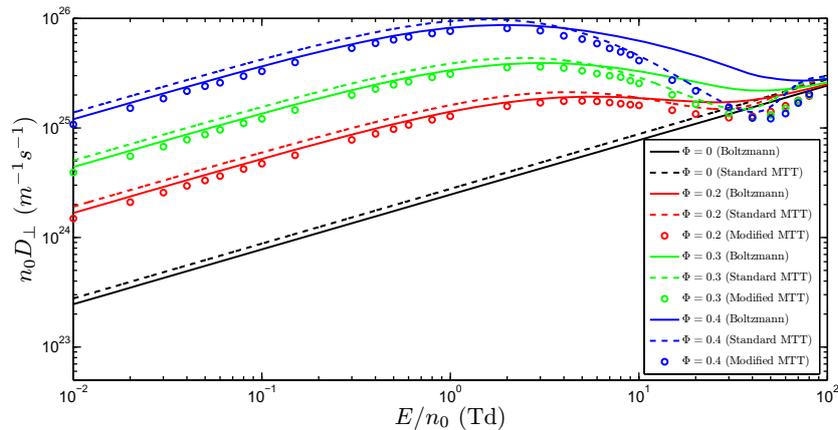

Figure 13. Variation of the transverse diffusion coefficient with reduced electric field for various volume fractions Φ for a dense gas of hard spheres. Fluid results are compared with those from a multi-term Boltzmann equation solution [1]. ——, $\Phi = 0$ (Boltzmann); - - - - $\Phi = 0$ (standard MTT); ——, $\Phi = 0.2$ (Boltzmann); - - - -, $\Phi = 0.2$ (standard MTT); ○, $\Phi = 0.2$ (modified MTT); ——, $\Phi = 0.3$ (Boltzmann); - - - -, $\Phi = 0.3$ (standard MTT); ○, $\Phi = 0.3$ (modified MTT); ——, $\Phi = 0.4$ (Boltzmann); - - - -, $\Phi = 0.4$ (standard MTT); ○, $\Phi = 0.4$ (modified MTT).

as expected. Although E_{eff} is calculated from the same expression, there are small differences evident between the standard and modified MTT results. This is due to (51) being evaluated at slightly different dilute gas phase energies, the former using an MTT calculation, while the latter uses the Boltzmann solution information directly. It is thus expected that modified MTT predictions are more accurate.

2.4.3. Diffusion coefficients. The diffusion coefficients can then be found from (32) and (37) using the homogeneous transport quantities as inputs, and are shown in figures 13 and 14. The diffusion coefficients found from the modified MTT are generally more accurate than the standard MTT, which is to be expected from using more accurate inputs. Phenomenologically, comments made in section 2.3.3 still apply here. A breakdown of the low-order fluid model entirely for the two largest-volume fractions, $\Phi = 0.3$ and $\Phi = 0.4$, in the region where the dense gas phase collision frequency varies sharpest with energy is again seen.

2.4.4. Liquid argon. We now apply the modified MTT technique to the case of positrons in liquid argon at 84 K.

2.4.5. Drift velocity and mean energy. Figure 15 details the variation of positron swarm mean energy with the reduced electric field in gaseous and liquid argon. Previously, when using the standard MTT approach, the mean energy exhibited peculiar, inaccurate and unphysical behaviour. Here the modified MTT approach yields results with accuracy comparable to the test hard sphere case. The dilute gas and liquid profiles also now converge at high field strengths. Although the effects of inelastic processes become significant at approximately 100 Td, the
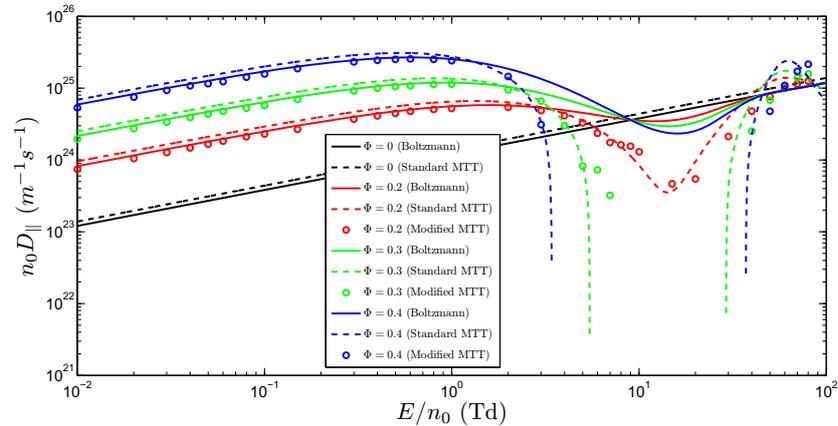
Figure 14. Variation of the longitudinal diffusion coefficient with reduced electric field for various volume fractions Φ for a dense gas of hard spheres. Fluid results are compared with those from a multi-term Boltzmann equation solution [1]. ——, $\Phi = 0$ (Boltzmann); - - - -, $\Phi = 0$ (standard MTT); ——, $\Phi = 0.2$ (Boltzmann); - - - -, $\Phi = 0.2$ (standard MTT); ○, $\Phi = 0.2$ (modified MTT); ——, $\Phi = 0.3$ (Boltzmann); - - - -, $\Phi = 0.3$ (standard MTT); ○, $\Phi = 0.3$ (modified MTT); ——, $\Phi = 0.4$ (Boltzmann); - - - -, $\Phi = 0.4$ (standard MTT); ○, $\Phi = 0.4$ (modified MTT).
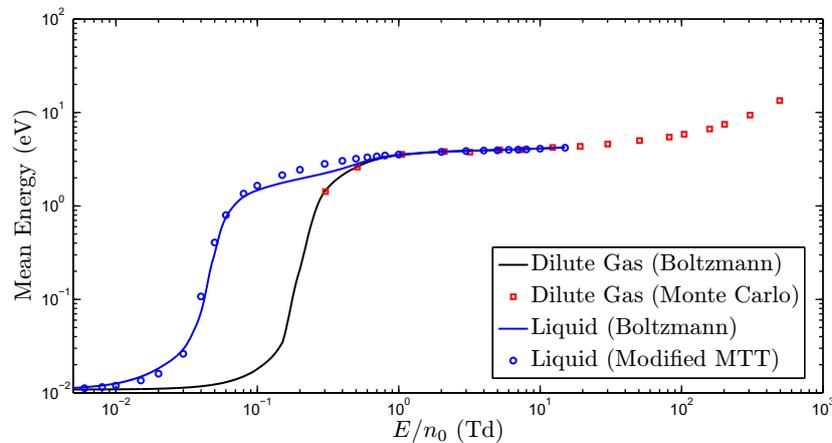

Figure 15. Variation of the swarm mean energy with reduced electric field for dilute gaseous and liquid argon at 84 K. Fluid results are compared with those from a multi-term Boltzmann equation solution [1] and Monte Carlo simulation [21]. ——, Dilute gas (Boltzmann); ○, dilute gas (modified MTT); □, dilute gas (Monte Carlo); ——, liquid (Boltzmann); ○, liquid (modified MTT).

inaccuracies that one would expect from neglecting inelastic processes are suppressed in figure 15 by the collision frequency fitting process. This is somewhat fortuitous as the coherent scattering effects are becoming suppressed in this region, and the approximation of a coherent effective collision frequency model is minimized.
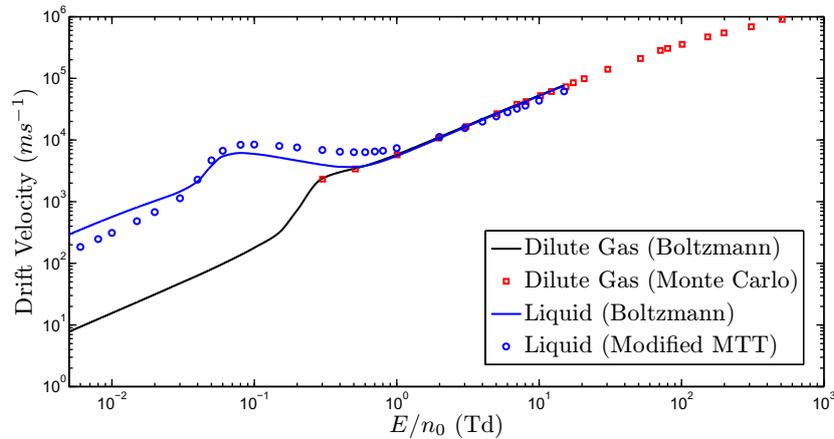
Figure 16. Variation of the swarm flux drift velocity with reduced electric field for dilute gaseous and liquid argon at 84 K. Fluid results are compared with those from a multi-term Boltzmann equation solution [1] and Monte Carlo simulation [21]. ——, Dilute gas (Boltzmann), ○ dilute gas (modified MTT), □ dilute gas (Monte Carlo), —— liquid (Boltzmann), ○ liquid (modified MTT).
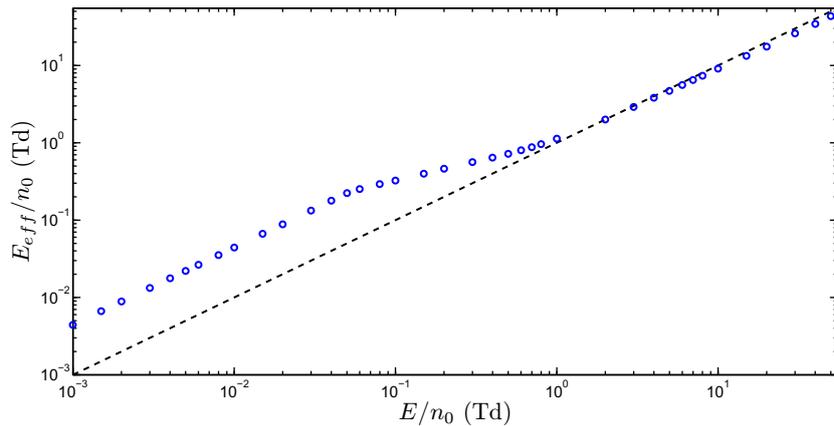

Figure 17. Variation of the reduced effective electric field, E_{eff}, with reduced electric field for dilute gaseous and liquid argon at 84 K. Fluid results are compared with those from a multi-term Boltzmann equation solution [1] and Monte Carlo simulation [21].

The variation of the drift velocity with reduced electric field is highlighted in figure 16. The new model used to obtain liquid phase drift velocities from the dilute gas phase drift velocities is shown to produce the required qualitative behaviour, again successfully demonstrating structure-induced NDC. The accuracy is generally within the 10–20% expected from using an MTT approximation. The discrepancy in the low field region is, we believe, a consequence of different extrapolation methods used by the Boltzmann and fluid numerical algorithms to evaluate the structure factor and process cross-sections at low energies.

The relationship between the actual reduced electric field strength and effective reduced electric field for liquid argon is shown in figure 17. The largest difference between the two
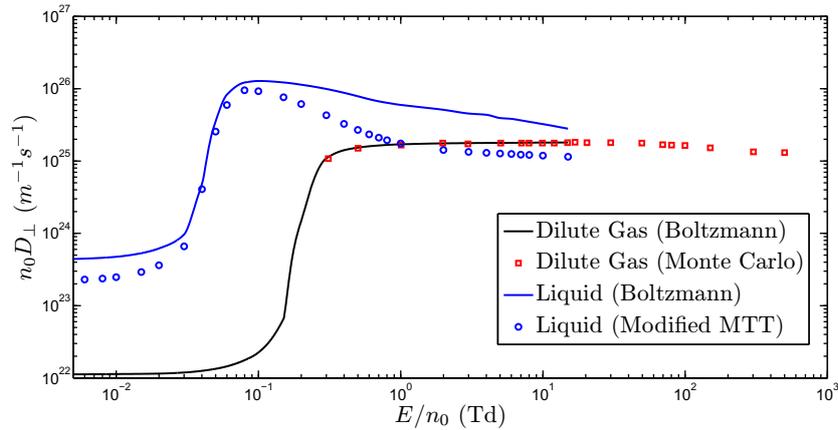
Figure 18. Variation of the transverse diffusion coefficient with reduced electric field for dilute gaseous and liquid argon at 84 K. Fluid results are compared with those from a multi-term Boltzmann equation solution [1] and Monte Carlo simulation [21]. ——, Dilute gas (Boltzmann); ○ , dilute gas (modified MTT); □, dilute gas (Monte Carlo); ——, liquid (Boltzmann); ○ , liquid (modified MTT).
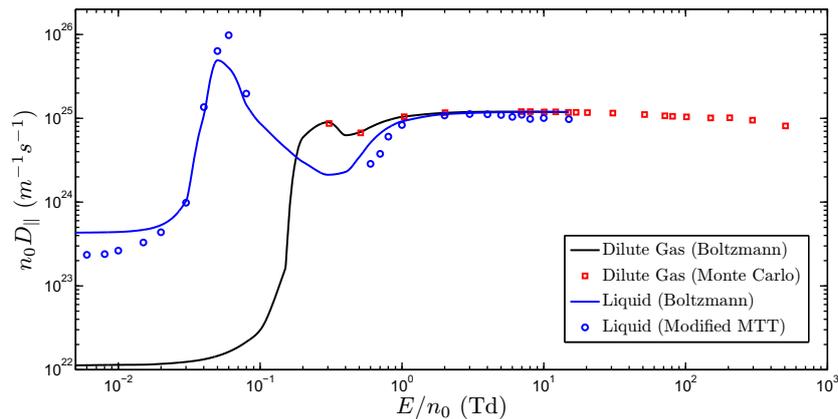

Figure 19. Variation of the longitudinal diffusion coefficient with reduced electric field for dilute gaseous and liquid argon at 84 K. Fluid results are compared with those from a multi-term Boltzmann equation solution [1] and Monte Carlo simulation [21]. ——, Dilute gas (Boltzmann); ○ , dilute gas (modified MTT); □, dilute gas (Monte Carlo); ——, liquid (Boltzmann); ○ , liquid (modified MTT).

profiles occurs at the lowest field strengths, which then converge as the field increases as required. Again the effective field is generally greater than the actual, reflecting the mostly increased mean energy and drift velocity exhibited by swarms in the liquid phase in figures 15 and 16, reflecting the enhanced efficiency of the field in pumping energy into the swarm due to the reduced momentum exchange associated with coherent scattering.

2.4.6. Diffusion coefficients. The variation of the transverse and longitudinal diffusion coefficients with reduced electric field is detailed in figures 18 and 19. Although the accuracy

IOP Institute of Physics **Φ** DEUTSCHE PHYSIKALISCHE GESELLSCHAFT

of these higher-order quantities has decreased, the modified MTT approach still yields a good qualitative description of the liquid phase diffusion behaviour. Despite significant discrepancies between the predicted and expected transverse diffusion coefficients at high field strengths, the longitudinal diffusion coefficients do behave qualitatively well in this region. However, similar to the behaviour observed for the test hard sphere situation, for regions in which NDC occurs, our low-order MTT theory breaks down, as is evident from figure 19. Extra correction terms may once again need to be included to account for this.

3. Conclusion

Although there exist a wide variety of applications associated with electrons and positrons in structured and soft-condensed matter, the literature on experimental and theoretical transport properties in such systems is limited in comparison with its dilute gas phase counterpart. In this paper, we have discussed how the effects of coherent scattering in structured and soft-condensed matter can be included in a transport theory, adapting gas phase cross-sections through the inclusion of the spatial and temporal correlations of the scatterers via structure factors. A fluid model has been developed primarily to gain physical insight, as well as simplify computations, which generalizes many of the relations for dilute gas phase systems to soft-condensed systems, including the Wannier energy relation and the GER for diffusion. We have applied these relations to a benchmark model and to positrons in liquid argon, and compared favourably the results with a full multi-term Boltzmann solution [1, 27]. The low-order MTT approximation was shown to break down in argon, and a modified approach was developed using simple relations that evaluate soft-condensed phase transport properties from a knowledge of transport properties in the dilute gas phase and the structure factor of the medium. The modified fluid model relations provide excellent qualitative agreement and generally good quantitative agreement. Given the ease of implementation and ability to capitalize on the existing transport literature, the fluid models developed will be beneficial tools for predicting the transport properties in soft-condensed matter from the existing gas phase data.

References

[1] White R and Robson R 2011 *Phys. Rev.* E **84** 031125
[2] Schmidt W 1984 *IEEE Trans. Electr. Insul.* **E1–19** 389
[3] Tessler N, Preezant Y, Rappaport N and Roichman Y 2009 *Adv. Mater.* **21** 2741
[4] Cherry S, Sorensen J and Phelps M 2003 *Physics in Nuclear Medicine* (Philadelphia, PA: Saunders)
[5] Zheng Y, Wagner J R and Sanche L 2006 *Phys. Rev. Lett.* **96** 208101
[6] Nikjoo H, Emfietzoglou D, Watanabe R and Uehara S 2008 *Radiat. Phys. Chem.* **77** 1270–9
[7] Baibussinov B *et al* 2010 *J. Instrum.* **5** P03005
[8] Sakai Y 2007 *J. Phys. D: Appl. Phys.* **40** R441
[9] Cohen M and Lekner J 1967 *Phys. Rev.* **158** 305

IOP Institute of Physics ⬥ DEUTSCHE PHYSIKALISCHE GESELLSCHAFT

[10] Hove L V 1954 *Phys. Rev.* **95** 249

[11] White R, Robson R, Dujko S and Li B 2009 *J. Phys. D: Appl. Phys.* **42** 194001

[12] Viehland L and Mason E 1975 *Ann. Phys.* **91** 499

[13] Robson R 1986 *J. Chem. Phys.* **85** 4486

[14] Robson R 1986 *J. Chem. Phys.* **88** 198

[15] Vrhovac S and Petrović Z 1995 *Phys. Rev.* E **53** 4012

[16] Tonks L 1937 *Phys. Rev.* **51** 744

[17] Wannier G 1953 *Bell Syst. Tech. J.* **32** 170

[18] Robson R, White R and Petrović Z 2005 *Rev. Mod. Phys.* **77** 1303

[19] Robson R 2006 *Introductory Transport Theory for Charged Particles in Gases* (Singapore: World Scientific)

[20] Mason E and McDaniel E 1988 *Transport Properties of Ions in Gases* (New York: Wiley)

[21] Suvakov M, Petrović Z, Marler J, Buckman S, Robson R and Malović G 2008 *New J. Phys.* **10** 053034

[22] Petrović Z, Dujko AB S, Marjanović S, Suvakov M, Malović G, Marler J, Buckman S, White R and Robson R 2010 *J. Phys. Conf. Ser.* **199** 012016

[23] Robson R, White R and Makabe T 1997 *Ann. Phys.* **261** 74

[24] Robson R E, Nicoletopoulos P, Li B and White R D 2008 *Plasma Sources Sci. Technol.* **17** 024020

[25] Nicoletopoulos P and Robson R E 2008 *Phys. Rev. Lett.* **100** 124502

[26] Petrović Z, Suvakov M, Nikitović Z, Dujko S, Sasić O, Jovanović J, Malović G and Stojanović V 2007 *Plasma Sources Sci. Technol.* **16** S1

[27] White R and Robson R 2009 *Phys. Rev. Lett.* **102** 230602

[28] Viehland L and Mason E 1978 *Ann. Phys.* **110** 287

[29] Kumar K, Skullerud H and Robson R 1980 *Aust. J. Phys.* **33** 343

[30] Ness K and Robson R 1986 *Phys. Rev.* A **34** 2185

[31] White R, Robson R and Ness K 1995 *Aust. J. Phys.* **48** 925

[32] Sakai Y, Tagashira H and Sakamoto S 1977 *J. Phys. D: Appl. Phys.* **10** 1035

[33] Tagashira H, Sakai Y and Sakamoto S 1977 *J. Phys. D: Appl. Phys.* **10** 1051

[34] Robson R 1984 *Aust. J. Phys.* **37** 35

[35] Brent R 1973 *Algorithms for Minimisation without Derivatives* (Englewood Cliffs, NJ: Prentice-Hall)

[36] Press W, Flannery B, Teukolsky S and Vetterling W 1992 *Numerical Recipes in FORTRAN: The Art of Scientific Computing* 2nd edn (Cambridge: Cambridge University Press)

[37] Banković A, Petrović Z L, Robson R E, Marler J P, Dujko S and Malović G 2009 *Nucl. Instrum. Methods Phys. Res.* B **267** 350

[38] Petrović Z, Crompton R and Haddad G 1984 *Aust. J. Phys.* **37** 23

[39] Verlet L and Weis J 1971 *Phys. Rev.* A **5** 939

[40] Megen W and Pusey P 1991 *Phys. Rev.* A **43** 5429

[41] Margenau H 1946 *Phys. Rev.* **69** 508